A microscopic model for phase transitions in traffic flow

2002 J. Phys. A: Math. Gen. 35 L31

(http://iopscience.iop.org/0305-4470/35/3/102)

INSTITUTE OF PHYSICS PUBLISHING JOURNAL OF PHYSICS A: MATHEMATICAL AND GENERAL

J. Phys. A: Math. Gen. **35** (2002) L31–L43 PII: S0305-4470(02)31206-X

LETTER TO THE EDITOR

A microscopic model for phase transitions in traffic flow

Boris S Kerner[1] **and Sergey L Klenov**[2]

[1] DaimlerChrysler AG, FT3/TN, HPC: E224, 70546 Stuttgart, Germany
[2] Moscow Institute of Physics and Technology, Department of Physics, 141700 Dolgoprudny, Moscow Region, Russia

Received 26 November 2001
Published 11 January 2002
Online at stacks.iop.org/JPhysA/35/L31

Abstract

A microscopic model for phase transitions in traffic flow is presented. The basic assumption of the model is that hypothetical homogeneous and stationary, i.e. 'equilibrium' states of the model cover a two-dimensional region in the flow–density plane. As in empirical observations, in the model moving jams do not spontaneously occur in free flow. Instead, the first-order phase transition to synchronized flow beginning at some density in free flow is realized. The moving jams emerge only in synchronized flow. As a result, the diagrams of patterns (states) both for a homogeneous road without bottlenecks and at on-ramps are qualitatively different from those found in other approaches at present. In particular, only one type of pattern occurs at on-ramps, if the flow rates to the on-ramp and on the road are high enough: in this *general* pattern synchronized flow occurs upstream of the on-ramp and wide moving jams spontaneously emerge in this synchronized flow.

PACS numbers: 89.40.+k, 47.54.+r, 64.60.Cn, 64.60.Lx

Diverse patterns, in particular moving jams, are observed in congested traffic flow (see reviews [1–3]). In models of the jams [1, 2], the multitude of hypothetical homogeneous and time-independent model states (the 'equilibrium' states for short) where all vehicles move with the same time-independent speed at the same distances between vehicles belongs to a curve in the flow–density plane. This curve is called the fundamental diagram. In this fundamental diagram approach, moving jams spontaneously occur in free flow if the density is gradually increased. In some models, in equilibrium states of very high density no moving jams can emerge.

The empirical study [4] shows that in congested traffic two different phases should be distinguished: 'synchronized flow' and 'wide moving jam'. Synchronized flow, which shows very complex behaviour [3], occurs most at a bottleneck, in particular at an on-ramp. Synchronized flow of higher vehicle speed can exist for a long time without an occurrence

of moving jams. Moving jams are likely to occur in synchronized flow of high density and low vehicle speed, i.e. when a strong compression of synchronized flow is realized ('the pinch effect' in synchronized flow) [5].

A moving jam is an upstream moving localized structure which is restricted by two fronts where the vehicle speed changes sharply. The distance between the fronts of a *wide* moving jam is noticeably higher than the length of the jam fronts. An objective criterion for the identification of wide moving jams is [3, 6] the following: a wide moving jam *propagates* through either free or synchronized flows and through any bottlenecks (e.g. at on-ramps) *keeping* the velocity of the jam's downstream front. In contrast, after synchronized flow has occurred at a bottleneck, the downstream front of the synchronized flow is usually *fixed* at the bottleneck.

Moving jams do not emerge in free flow, if synchronized flow is not hindered [7]. Instead, the jams emerge due to a sequence of two first-order phase transitions [5]: first the transition from free flow to synchronized flow occurs (it will be called the F $\rightarrow$ S transition) and only later and usually at a different location moving jams emerge in the synchronized flow (the latter transition will be called the S $\rightarrow$ J transition and the sequence of both transitions the F $\rightarrow$ S $\rightarrow$ J transitions).

Different explanations of these empirical features of wide moving jams and synchronized flow which have been made during recent years are to date being discussed by different groups (e.g. [8–17] and the reviews [1, 2]).

In this Letter another approach to an explanation and to a microscopic traffic flow modelling of these phenomena is presented. In this approach, which is based on empirical observations [3–5] and on the hypotheses of the three-phase-traffic theory [3, 5, 18], there is *no* fundamental diagram for equilibrium states of a microscopic model: the multitude of *equilibrium states* of synchronized flow in the model belongs to a two-dimensional region in the flow–density plane (figure 1(a)).

The two-dimensional region of the equilibrium states in the flow–density plane (figure 1(a)) is restricted by three boundaries: the upper (line U), the lower (line L) and the left (line F) boundaries. The upper boundary U is determined implicitly by the safe speed v_s, which depends on the front-to-front distance dx and on the vehicle speed v:

$$v^{(h)} = v_s^{(h)}(dx^{(h)}, v^{(h)}). \tag{1}$$

The lower boundary L is determined by the maximal distance D at which the vehicle takes into account the speed of the leading vehicle when accelerating:

$$dx^{(h)} = D^{(h)}(v^{(h)}). \tag{2}$$

The left boundary F corresponds to the maximal speed v_{free} in free flow which is assumed to be the same for all vehicles. Here and below the upper index h marks functions related to equilibrium states (homogeneous in space and time-independent states)

$$v_i = v^{(h)} \qquad dx_i = dx^{(h)}; \tag{3}$$

the index i corresponds to the discrete time $t = i\tau$, $i = 0, 1, 2, \ldots$; τ is the time step; $dx_i = x_{\ell,i} - x_i$; v_i and x_i are the speed and the space co-ordinate of the vehicle; the lower index ℓ marks functions (or values) related to the leading vehicle.

The model provides the two-dimensional region of equilibrium speeds between these boundaries due to the use of the following rules of vehicle motion:

$$v_{i+1} = \min(v_{free}, v_{c,i}, v_{s,i}) \qquad x_{i+1} = x_i + v_{i+1}\tau \tag{4}$$

$$v_{c,i} = \begin{cases} v_i + \Delta_i & \text{at} \quad dx_i \leqslant D_i \\ v_i + a_i\tau & \text{at} \quad dx_i > D_i \end{cases} \tag{5}$$

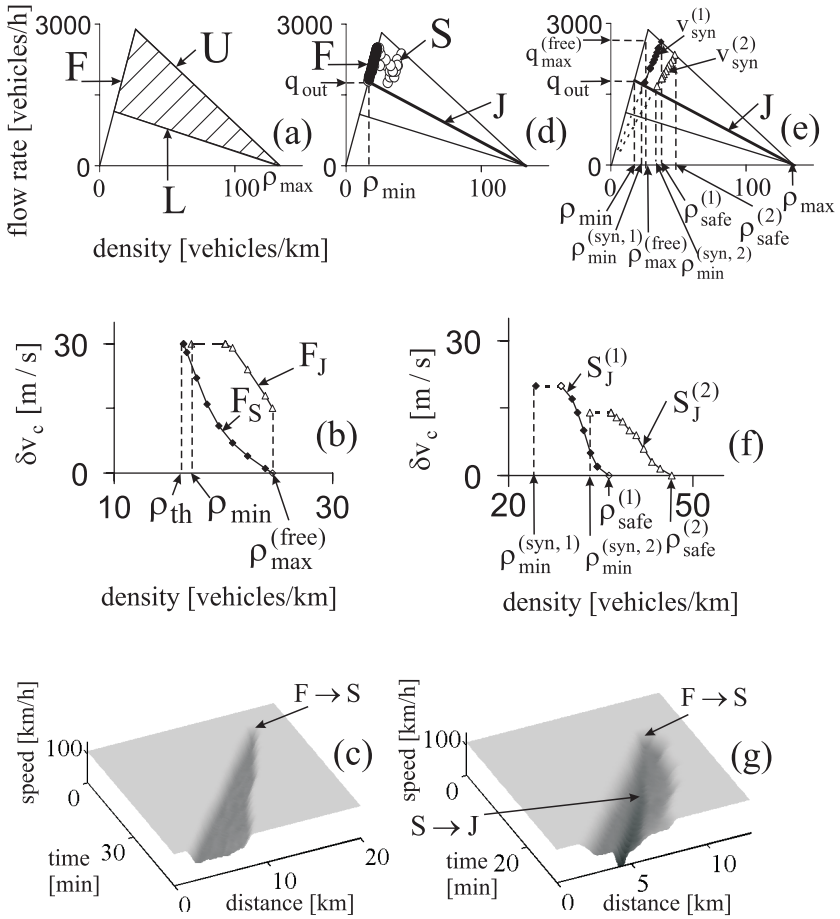

Figure 1. The equilibrium states of the model in the flow–density plane (*a*) and phase transitions on the road without bottlenecks (*b*)–(*g*). Parts (*d*) and (*e*) explain the phase transitions in the flow–density plane. Parts (*b*) and (*f*) show the dependences of the critical amplitude of local perturbations on the density for the F $\to$ J transition (curve F_J), for the F $\to$ S transition (curve F_S) and for the S $\to$ J transition (curves $S_J^{(1)}$ and $S_J^{(2)}$). Parts (*c*) and (*g*) show the phase transitions and the related development of congested patterns in space and in time. Initial local perturbations used for the study of the phase transitions (*b*)–(*g*) are caused by a braking of one of the vehicles with constant deceleration 1 m s^{-2} during a finite time, which implies the decrease in the speed of this vehicle δv being chosen as the amplitude of the local perturbation. The parameters of the initial local perturbations in (*c*) and (*g*) are the location $x_0 = 16$ km (*c*) and $x_0 = 10$ km (*g*), the begin time $t_0 = 10$ min, the amplitude $\delta v = 20$ m s^{-1}; the initial flow rates are $q_{\rm in} = 2320$ and 2480 vehicles/h per lane for (*c*) and (*g*), respectively. In (*c*) and (*g*) the vehicle speed is averaged over the group of ten subsequent vehicles and over two road lanes.

where $D_i = D(v_i, v_{\ell,i})$; $v_{{\rm s},i}$ is the time-dependent safe speed; a_i is the acceleration;

$$\Delta_i = \begin{cases} -f_i & \text{if} \quad v_i > v_{\ell,i} \\ 0 & \text{if} \quad v_i = v_{\ell,i} \\ c_i & \text{if} \quad v_i < v_{\ell,i} \end{cases} \tag{6}$$

where $f_i \geqslant 0, c_i \geqslant 0$.

Whereas in models characterized by a fundamental diagram (e.g. [8, 9, 11–17] and the reviews [1, 2]) a vehicle would close up to the leading one adapting its velocity and gap as required by secure driving, the new feature of the present model is the introduction of the distance D, within which the drivers adapt their velocity to that of the leading vehicle without caring what their precise gap is, as long as it is safe. This explains why there is no unique flow–density relationship in the present model. Indeed, on the one hand, in an equilibrium state (3) $v_i = v_{\ell,i} = v^{(h)}$, therefore according to (6) $\Delta_i = 0$. On the other hand, in an equilibrium state (3) the functions D_i and $v_{s,i}$ in (4) and (5) do not depend on time; i.e., $D_i = D^{(h)}(v^{(h)})$, $v_{s,i} = v_s^{(h)}(\mathrm{d}x^{(h)}, v^{(h)})$. Using these conditions one finds from (4) and (5) that $v_{c,i} = v_i$ and consequently $v_{i+1} = v_i$, i.e., the speed does not depend on time, when the following conditions are fulfilled:

$$\mathrm{d}x^{(h)} \leqslant D^{(h)}(v^{(h)}) \qquad v^{(h)} \leqslant v_s^{(h)}(\mathrm{d}x^{(h)}, v^{(h)}) \qquad v^{(h)} \leqslant v_{\mathrm{free}}. \tag{7}$$

Thus, from the motion rules (4)–(6) it follows that there is a multitude of equilibrium states in the model which is determined by the conditions (7). This multitude corresponding to (1) and (2) indeed covers the two-dimensional region in the flow–density plane between the lines F, U and L in figure 1(*a*). This means that a given equilibrium speed is related to an infinite multitude of the vehicle densities between the boundaries U and L in figure 1(*a*) and consequently a given density is related to an infinite multitude of equilibrium speeds.

The conditions (4)–(6) are the basis of the model. All results below are derived with the following specific functions, which complete the model (4)–(6): for the safe speed in (4)

$$v_{s,i} = \min\,(V_i,\ \tau^{-1}(\mathrm{d}x_i - d) + V_{\ell,i}) \tag{8}$$

for the distance D in (5)

$$D(v_i, v_{\ell,i}) = d + \max(0, kv_i\tau + a_0^{-1}v_i(v_i - v_{\ell,i})) \tag{9}$$

for the vehicle deceleration in (6)

$$f_i = \min\,(f_i^{(\mathrm{dyn})} + f_i^{(r)},\ b_0\tau) \tag{10}$$

and acceleration in (6)

$$c_i = \min\,(c_i^{(\mathrm{dyn})} + c_i^{(r)},\ a_i\tau) \tag{11}$$

where

$$f_i^{(dyn)} = \begin{cases} \beta(v_i - v_{\ell,i}) & \text{if} \quad B_{\ell,i} = 1 \quad \text{and} \quad r_1 < p_1 \\ & \text{or} \quad B_i = 1 \quad \text{and} \quad r_1 < p_2 \\ 0 & \text{otherwise} \end{cases} \tag{12}$$

$$c_i^{(dyn)} = \begin{cases} \alpha(v_{\ell,i} - v_i) & \text{if} \quad B_{\ell,i} = 0 \\ 0 & \text{otherwise} \end{cases} \tag{13}$$

$$f_i^{(r)} = \begin{cases} b_0\tau & \text{if} \quad r_2 < p_b \quad \text{and} \quad (f_i^{(\mathrm{dyn})} > 0 \text{ or } v_{s,i} < v_i) \\ 0 & \text{otherwise} \end{cases} \tag{14}$$

$$c_i^{(r)} = \begin{cases} a_i\tau & \text{if} \quad r_2 < p_a \quad \text{and} \quad c_i^{(\mathrm{dyn})} > 0 \\ 0 & \text{otherwise} \end{cases} \tag{15}$$

$$a_i = \begin{cases} a_0 & \text{if} \quad r_1 \geqslant p_0 \quad \text{or} \quad v_i > v_{i-1} \\ 0 & \text{otherwise} \end{cases} \tag{16}$$

where $V_i = v_{\mathrm{safe}}(\mathrm{d}x_i, v_{\ell,i})$, v_{safe} is taken from [12] ((3)–(5) in [12] with the deceleration $b = 1\ \mathrm{m\ s^{-2}}$ and the gap $g = \mathrm{d}x_i - d$); d is the vehicle length; $B_{i+1} = 1$ if $v_{i+1} < v_i - \delta$ and

$B_{i+1} = 0$ if $v_{i+1} \geqslant v_i - \delta$; α, β, k, a_0, b_0, p_1, p_a, p_b and δ are model parameters; $p_0 = p_0(v_i)$ and $p_2 = p_2(v_i)$ are considered as vehicle speed functions; r_1 and r_2 are independent random values uniformly distributed between zero and unity; in (8), (12) and (13) the ideas of an estimation of the safe speed of the leading vehicle and of the brake-light and its status B_i [14, 15] are used; the functions $f_i^{(\mathrm{dyn})}$ (12) and $c_i^{(\mathrm{dyn})}$ (13) describe the smooth adaptation of the vehicle speed to that of the leading vehicle whereas the functions $f_i^{(r)}$ (14) and $c_i^{(r)}$ (15) give the fluctuations when the vehicle decelerates or accelerates, respectively; the slow-to-start rules [16] are used in (16)—vehicles escape at the downstream front of a wide moving jam with the mean delay time $\tau_{\mathrm{del}} = \tau/(1 - p_0(0))$, which as well as in [15] provides the jam propagation through free and synchronized flows with the same velocity of the jam downstream front v_g, that corresponds to a qualitative theory and to the related formula $v_g = 1/(\rho_{\max}\tau_{\mathrm{del}})$ from [5]; $\rho_{\max}$ is the density inside the jam.

For the case of a two-lane highway where vehicles may change lane the known incentive and security conditions [17], which have been modified for the present model with continuous changes in the vehicle speed, are used. The following conditions for the lane change from the right-hand lane to the left lane (R $\to$ L) and a return (L $\to$ R) are taken:

$$\mathrm{R} \to \mathrm{L}: \ v_i^+ \geqslant v_{\ell,i} + \delta_1 \qquad \text{and} \qquad v_i \geqslant v_{\ell,i} \tag{17}$$

$$\mathrm{L} \to \mathrm{R}: \ v_i^+ > v_{\ell,i} + \delta_2 \qquad \text{or} \quad v_i^+ > v_i + \delta_2, \tag{18}$$

$$\mathrm{d}x_i^+ > \min(\gamma^+ v_i \tau + d, \ D^+) \qquad \mathrm{d}x_i^- > \min(\gamma^- v_i^- \tau + d, \ D^-) \tag{19}$$

where $D^+ = D(v_i, v_i^+)$, $D^- = D(v_i^-, v_i)$; $\delta_1 \geqslant 0$, $\delta_2 \geqslant 0$, γ^+ and γ^- are constants; the upper index + (−) belongs to the vehicle on the target lane ahead (behind) the vehicle that wants to change the lane; $\mathrm{d}x_i^+$ ($\mathrm{d}x_i^-$) is the distance between this vehicle and the vehicle ahead (behind). At $\delta_1 = 0$ the incentive conditions (17) and (18) are the 'hypothetical American rules with slack' (δ_2) used in cellular automata models [17]. Since the present model is the model with continuous changes in the vehicle speed, the finite speed difference $\delta_1 = \delta_2$ is used in criterion (17). In addition, similarly to [17], the speed v_i^+ ($v_{\ell,i}$) in (17) and (18) is set to ∞ if the distance $\mathrm{d}x_i^+$ ($\mathrm{d}x_i$) exceeds the look-ahead distance L_{a} equal to 150 m. The conditions (19) taken without the functions D^+, D^- are the usual security conditions used in different multi-lane models [17]. The functions D^+, D^- in (19) facilitate the synchronization of the vehicle speed across the lanes in the dense flow. If the conditions (17)–(19) are fulfilled, then also in [19] in the model the vehicle changes lane with the probability p_{c}.

A numerical study of the model (4)–(6), (8)–(19) is made for two cases: the homogeneous (without bottlenecks) two-lane road with cyclic and open boundary conditions (figures 1(*b*)–(*g*)) and the two-lane road with an on-ramp (open boundary conditions) (figures 2 and 3). For simulation of the on-ramp two consecutive vehicles on the right-hand lane of the road within the on-ramp area are chosen randomly and the entering vehicle is placed at equal distances between them, taking the speed of the leading vehicle v^+ [13]. The additional condition was that the distance between two consecutive vehicles on the right-hand lane should exceed some value $\lambda v^+ \tau + 2d$, where the parameter λ characterizes the behaviour of entering vehicles ($\lambda = 0$ corresponds to the most aggressive behaviour).

In a numerical study of the model (figures 1–3) the following parameters have been used: $d = 7.5$ m, $v_{\mathrm{free}} = 30$ m s^{-2}, $\tau = 1$ s, $a_0 = b_0 = 0.5$ m s^{-2}, $\alpha = \beta = 1$, $k = 3.5$, $\delta = 0.01$, $p_1 = 0.4$, $p_a = 0.15$, $p_b = 0.1$, $p_2(v) = 0.5 + 0.3\theta(v - 15)$, where $\theta(z) = 1$ if $z \geqslant 0$ and $\theta(z) = 0$ if $z < 0$, $p_0(v) = 0.3 + 0.125\max(0, 1 - v/10)$, $p_{\mathrm{c}} = 0.45$, $\delta_2 = 2a_0\tau$, $\gamma^+ = 1$, $\gamma^- = 0.5$ and $\lambda = 0.5$. The on-ramp starts at 16 km from the beginning of the 20 km long road and its merging area was 0.3 km long. The study allows us to draw the conclusions presented below.

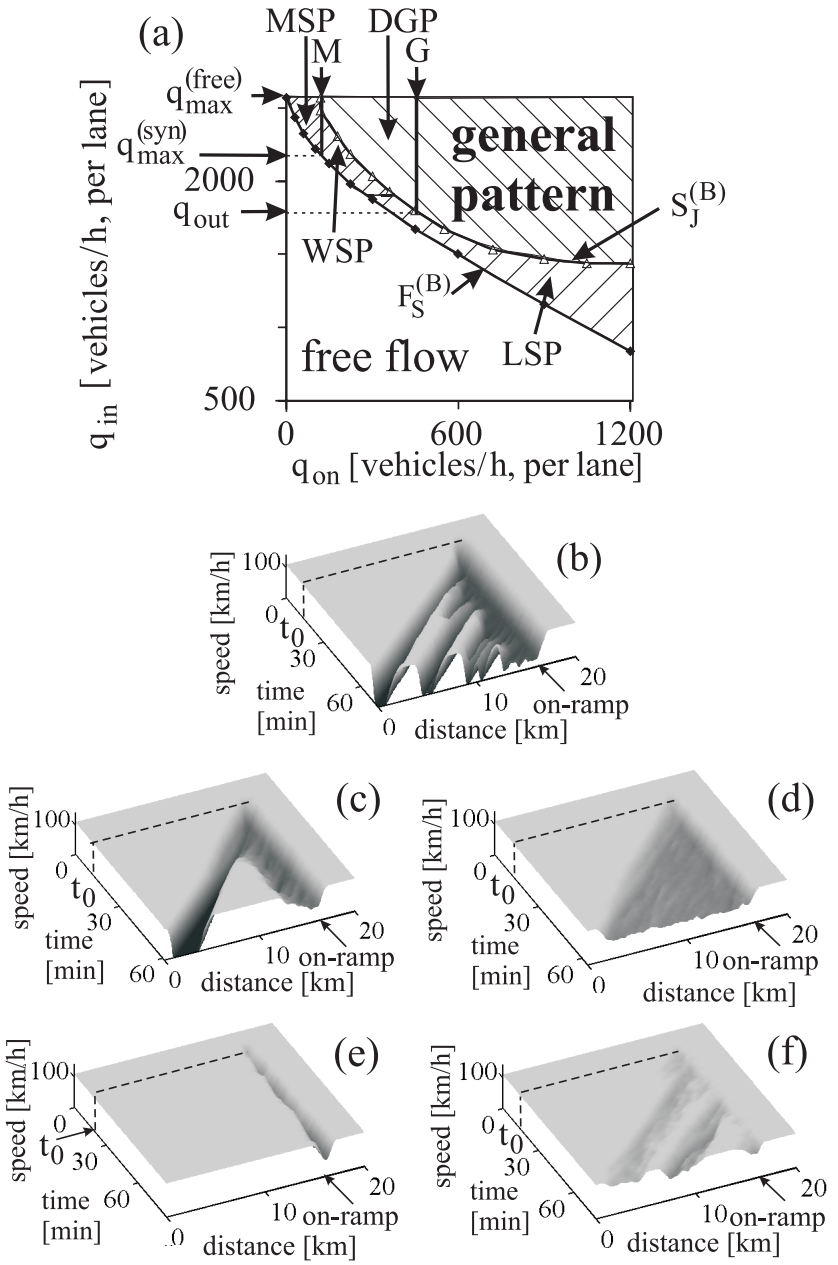

Figure 2. The diagram of congested patterns at on-ramps (*a*), the general pattern (GP) (*b*), the dissolving general pattern (DGP) (*c*), the widening synchronized flow pattern (WSP) (*d*), the localized synchronized flow pattern (LSP) (*e*) and the moving synchronized flow pattern (MSP) (*f*). In (*b*)–(*f*) at $t_0 = 10$ min the on-ramp inflow is switched on; the flow rates (q_{on}, q_{in}) have the following values: (*b*) (600, 2000), (*c*) (290, 2290), (*d*) (180, 2290), (*e*) (480, 1675) and (*f*) (75, 2290) vehicles/h per lane. In (*b*)–(*f*) the vehicle speed is averaged over the group of ten subsequent vehicles and over two road lanes.

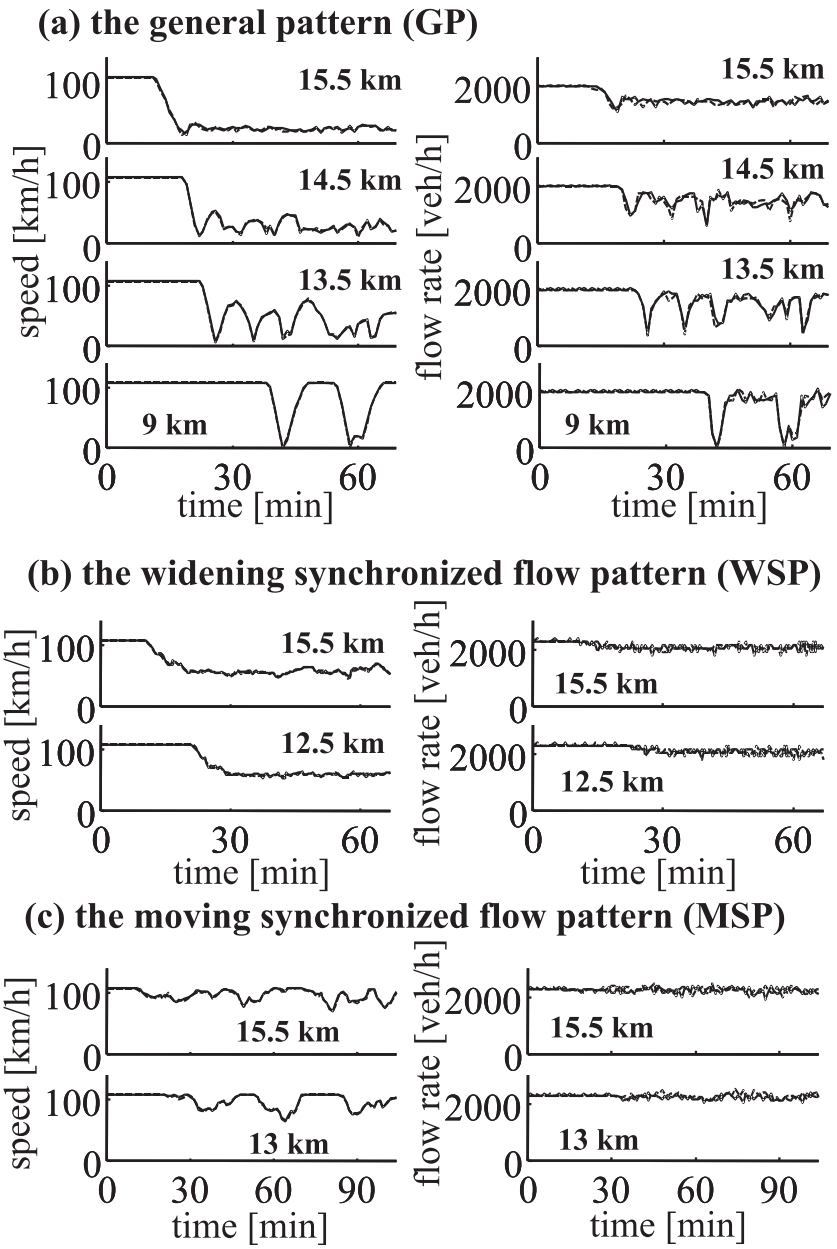

Figure 3. The vehicle speed (left) and the flow rate (right) for the GP (*a*) shown in figure 2(*b*), for the widening synchronized flow pattern (*b*) shown in figure 2(*d*) and for the moving synchronized flow pattern (*c*) shown in figure 2(*f*). One minute averaged data of virtual detectors whose coordinates are indicated in (*a*)–(*c*). The on-ramp is at $x = 16$ km. Data are shown for both road lanes.

(i) *On a homogeneous two-lane road* (without bottlenecks), phase transitions and congested patterns show the following spatial–temporal nonlinear features (1)–(5).

(1) The F $\rightarrow$ S transition is the first-order phase transition. If a local perturbation occurs in an initial free flow this perturbation grows leading to the F $\rightarrow$ S transition only if the amplitude of the perturbation δv exceeds some critical value, δv_{c}, otherwise the perturbation gradually

dissolves and the initial free flow is recovered (the nucleation effect). The critical amplitude of the local perturbation δv_c is a decreasing function of the density in free flow (the curve F_S in figure 1(*b*)). The critical amplitude δv_c reaches the maximum value at the threshold density for the F $\rightarrow$ S transition, ρ_{th}, and it is zero at the maximal density in free flow $\rho_{max}^{(free)}$, which is related to the maximal flow rate in free flow $q_{max}^{(free)}$. If the density is lower than ρ_{th}, no F $\rightarrow$ S transitions can be induced by the chosen local perturbation.

After the F $\rightarrow$ S transition has occurred, a further spacetime evolution of a region of synchronized flow inside an initially free flow is shown in figure 1(*c*). The circle points S in figure 1(*d*) which are related to this synchronized flow (measured at the location 11.5 km and then averaged during 30 s intervals) show that this synchronized flow belongs to 'homogeneous-in-speed' synchronized flow where the speed is nearly constant ($\approx$55 km h^{-1}) and the density changes over space and time. If the initial density is close to the threshold density for the F $\rightarrow$ S transition, ρ_{th}, the region of synchronized flow does not expand (in contrast to figure 1(*c*)) and can dissolve in about 5–10 min due to the self-fluctuations in the model.

(2) At any density of free flow moving jams do *not* spontaneously occur. In free flow above the threshold density ρ_{min} for the F $\rightarrow$ J transition (the phase transition from free flow to a wide moving jam), the jams can only be excited if an initial local perturbation of a very large amplitude is applied. This amplitude should be higher than the critical amplitude of the local perturbation for the F $\rightarrow$ J transition (curve F_J in figure 1(*b*)). The density ρ_{min} is related to the flow rate $q_{out} = 1810$ vehicles h^{-1} in the outflow of a wide moving jam (for the case when free flow is formed downstream of the wide moving jam).

As in [4] the velocity of the downstream front of a wide moving jam v_g is the characteristic, i.e. unique, predictable and reproducible, parameter, which is a constant for given model parameters. This velocity together with the threshold point, ρ_{min}, q_{out}, determine the characteristic line J for the downstream front of a wide moving jam (line J in figures 1(*d*) and (*e*)).

If the initial density in free flow is only slightly higher than ρ_{min} (dotted part of the curve F_J in figure 1(*b*)), after the maximal possible amplitude of the critical perturbation leading to a stop of the vehicle is chosen, it is necessary to maintain this stop for some further time (about 2–3 min at ρ_{min}) for the F $\rightarrow$ J transition in free flow.

(3) At any density in free flow the critical amplitude of the local perturbation needed for the F $\rightarrow$ J transition (curve F_J in figure 1(*b*)) is considerably higher than that for the F $\rightarrow$ S transition (curve F_S): at any density in free flow fluctuations can cause only the F $\rightarrow$ S transition rather than the F $\rightarrow$ J transition (figure 1(*b*)). Thus, in our model the diagram of patterns on the homogeneous road is qualitatively different from those in other approaches [1, 2].

(4) Line J determines the threshold of the moving jam excitation in synchronized flow. All densities in equilibrium synchronized flows related to line J are threshold densities with respect to the jam formation (the S $\rightarrow$ J transition) (e.g. $\rho_{min}^{(syn,\ 1)}$ and $\rho_{min}^{(syn,\ 2)}$ are the threshold densities for the speeds $v_{syn}^{(1)} = 72$ km h^{-1} and $v_{syn}^{(2)} = 51$ km h^{-1}, respectively, figure 1(*e*)). At the same speed, the higher the density is, the lower the critical amplitude δv_c of a local perturbation for the S $\rightarrow$ J transition is (curves $S_J^{(1)}$ and $S_J^{(2)}$ for the speeds $v_{syn}^{(1)}$ and $v_{syn}^{(2)}$, respectively, figure 1(*f*)). The critical amplitude δv_c for the S $\rightarrow$ J transition reaches the maximum value at the threshold density. At the same difference between the initial density and the threshold density, the lower the initial speed is, the lower the critical amplitude δv_c is (compare curves $S_J^{(1)}$ and $S_J^{(2)}$).

(5) The latter result allows a simulation of the F $\rightarrow$ S $\rightarrow$ J transitions (figure 1(*g*)). If due to the F $\rightarrow$ S transition, which is caused by the local perturbation applied at some location, synchronized flow of a relatively low vehicle speed occurs, then the S $\rightarrow$ J transition occurs later spontaneously at another location.

(ii) *On the two-lane road with the on-ramp*, depending on the flow rate to the on-ramp q_{on} and on the flow rate on the highway upstream of the on-ramp q_{in}, different congested patterns are possible. The related diagram of the patterns at on-ramps is shown in figure 2(*a*). The study of these patterns allows us to make the pattern classification and to find their spatial–temporal features in (1)–(8) below.

(1) Right of the boundary $S_J^{(B)}$ and of line G a congested pattern occurs where synchronized flow appears upstream of the on-ramp and wide moving jams spontaneously emerge in that synchronized flow. Because this pattern consists of both traffic phases in congested traffic ('synchronized flow' and 'wide moving jam') this pattern will be called 'the general pattern' or 'GP' for short (figure 2(*a*)).

At high enough flow rates q_{on} and q_{in} the GP consists of two parts (figure 2(*b*)):

(a) the spatial–temporal pattern of synchronized flow which is upstream bordered by

(b) a sequence of wide moving jams, or the region of wide jams for short.

This GP resembles the pattern studied in empirical observations [5]. Indeed, as in [5], in the synchronized flow the pinch effect is realized where the vehicle density is high and the vehicle speed is low. In the pinch region, growing narrow moving jams emerge (figures 2(*b*) and 3(*a*)). At the upstream boundary (front) of the synchronized flow some of these narrow jams transform into wide moving ones; i.e., the S $\rightarrow$ J transition occurs. The successive process of the transformation of narrow moving jams into wide moving jams at the upstream boundary of synchronized flow leads to the formation of the region of wide jams. The upstream boundary of this region is related to the upstream front of the most upstream wide jam. The mean time distance between the downstream fronts of wide moving jams is considerably higher than the mean time distance between narrow moving jams in the pinch region (18 min at the location 9 km and about 5.5 min at the locations 14.5–15.5 km in figures 2(*b*) and 3(*a*)).

Due to the upstream wide jam propagation, the region of wide jams is continuously widening upstream. Between wide moving jams either synchronized flow or free flow is formed. Nevertheless, the velocity of the downstream front of wide moving jams v_g remains constant ($v_g = -15.5$ km h^{-1} in figure 2(*b*)).

(2) At a given flow rate q_{in} in the whole region of the GP (right of the boundary $S_J^{(B)}$ and of line G) the GP does *not* transform into another type of pattern if the flow rate to the on-ramp q_{on} continuously increases. This is true for the model even if very low values of λ (down to zero, an extremely aggressive driver behaviour) have been used.

(3) Below and left of the boundary $F_S^{(B)}$ free flow occurs at the on-ramp. Between the boundaries $F_S^{(B)}$ and $S_J^{(B)}$ congested patterns occur where, in contrast to GP, wide moving jams do not emerge in synchronized flow. These patterns consist of the synchronized flow upstream of the on-ramp only. Therefore such a congested pattern will be called 'the synchronized flow pattern' or 'SP' for short (figures 2(*d*)–(*f*)). The limit point of the boundary $F_S^{(B)}$ at $q_{on} = 0$ is related to the maximum flow rate in free flow where $q_{in} = q_{max}^{(free)}$ ($q_{max}^{(free)} = 2570$ vehicles h^{-1}, figure 1(*e*)).

It has been found out that at high flow rates q_{in} the flow rate in synchronized flow in SP is lower than q_{in} and therefore the region of the synchronized flow is widening over time (figure 2(*d*)). This widening SP will be called 'the widening synchronized flow pattern' or 'WSP' for short. At lower flow rates q_{in}, the region of the synchronized flow is not continuously widening over time: the region of synchronized flow remains localized at the on-ramp. This localized SP will be called 'the localized synchronized flow pattern' or 'LSP' for short (figure 2(*e*)).

In both of these synchronized flow patterns (WSP and LSP) (figures 2(*d*) and (*e*)) the vehicle density (30–40 vehicles km^{-1}) is usually lower and the speed (45–60 km h^{-1}) is usu-

ally higher than the related values inside the pinch region of GP (40–80 vehicles km^{-1} and 10–35 km h^{-1}) (compare the examples in figures 3(*a*) and (*b*)). WSP where a relatively high and sometimes nearly constant vehicle speed in synchronized flow is realized (figures 2(*d*) and 3(*b*)) may explain 'homogeneous-in-speed' states which have been found in empirical observations [3, 4].

(4) It is found out that the flow rate in any SP pinned at the on-ramp cannot exceed some characteristic value $q_{\max}^{(\mathrm{syn})}$, which for the chosen model parameters is $q_{\max}^{(\mathrm{syn})} \approx$ 2200 vehicles h^{-1}.

(5) Right of the boundary $F_S^{(B)}$ and left of line M (the region marked 'MSP' in figure 2(*a*)) the flow rate q_{in} in an initial free flow upstream of the on-ramp satisfies the condition $q_{\mathrm{in}} > q_{\max}^{(\mathrm{syn})}$ (figure 2(*a*)). The point where the line M intersects the curve $F_S^{(B)}$ is related to the flow rate q_{in}, which is equal to $q_{\max}^{(\mathrm{syn})}$. After SP has just appeared at the on-ramp, the flow rate directly upstream of the on-ramp decreases. This flow rate in SP pinned at the on-ramp cannot be higher than $q_{\max}^{(\mathrm{syn})}$.

Apparently for this reason, it is found out that rather than WSP right of the boundary $F_S^{(B)}$ and left of line M one or a sequence of moving SP(s) emerge upstream of the on-ramp. After the SP has emerged at the on-ramp, the SP comes off the on-ramp and transforms into a moving SP. This moving SP will be called 'the moving synchronized flow pattern' or 'MSP' for short (figures 2(*f*) and 3(*c*)). In the MSP both the upstream and the downstream fronts move upstream of the on-ramp; i.e., the MSP moves as a whole localized pattern upstream of the on-ramp. In the outflow from the MSP, i.e. downstream of the MSP and upstream of the on-ramp when the MSP is far enough from the on-ramp the free flow condition with some flow rate q_{free} occurs.

At given values q_{on} and q_{in} right of the boundary $F_S^{(B)}$ and left of line M two different scenarios have been found.

(a) The value q_{free} satisfies the following condition: the point (q_{on}, q_{free}) lies right of the boundary $F_S^{(B)}$ and left of line M in figure 2(*a*), where instead of the initial flow rate q_{in} the value q_{free} is used in the diagram of congested patterns. Under this condition a new SP emerges at the on-ramp. This SP comes off the on-ramp later, and so on. In this case, a sequence of two or more MSPs emerge at the on-ramp (figures 2(*f*) and 3(*c*)).

(b) The point (q_{on}, q_{free}) mentioned in (a) lies left of the boundary $F_S^{(B)}$ in figure 2(*a*). In this case, the free flow condition remains at the on-ramp as long as $q_{\mathrm{free}} < q_{\max}^{(\mathrm{syn})}$ and the flow rate upstream of the on-ramp is determined by the outflow from this MSP only.

In contrast to a wide moving jam, inside the MSP both the vehicle speed (60–90 km h^{-1}) and the flow rate are high. Usually the flow rate inside the MSP is $q_{\mathrm{MSP}} \approx$ 2100–2200 vehicles h^{-1}; i.e., q_{MSP} is higher even than the flow rate in the free flow in the outflow from a wide moving jam $q_{\mathrm{out}} = 1810$ vehicles h^{-1}. Besides, the velocity of the downstream front of the MSP v_{MSP} is not a characteristic parameter. This velocity can change from about -10 to -25 km h^{-1} in the process of the MSP propagation or for different MSPs.

In some cases it has been found out that after the MSP is far away from the on-ramp, the pinch effect (the self-compression of synchronized flow) occurs inside the MSP and a wide moving jam can be formed there.

(6) Right of the boundary $S_J^{(B)}$ the pinch region is formed in the synchronized flow and moving jams spontaneously emerge in that synchronized flow upstream of the on-ramp. This leads to the GP formation (figure 2(*b*)). However, right of the boundary $S_J^{(B)}$ and left of line G (the region marked 'DGP' in figure 2(*a*)) in an initial free flow upstream of the on-ramp the flow rate q_{in} satisfies the condition $q_{\mathrm{in}} > q_{\mathrm{out}}$, where q_{out} is the flow rate in the outflow of a wide moving jam. The point where line G intersects the curve $S_J^{(B)}$ is related to the flow

rate q_{in}, which is equal to q_{out}. Thus, after a wide moving jam in synchronized flow has been formed, the initial condition $q_{\text{in}} > q_{\text{out}}$ can no longer be satisfied because the flow rate in the jam outflow cannot be higher than q_{out}.

This may explain the result that right of the boundary $S_J^{(B)}$ and left of line G (figure 2(*a*)) the GP dissolves during a relatively short time after it has first emerged. This short-living pattern will be called the 'dissolving general pattern' or 'DGP' for short (figure 2(*c*)). As a result of the dissolving of the GP, one or several traffic jams moving upstream occur, and one of the SPs (either WSP or LSP, figures 2(*d*), (*e*)) may be formed upstream of the on-ramp. In the outflow of wide moving jams the free flow is formed that separates the jams and SP at the on-ramp (figure 2(*c*)). In some cases due to S $\rightarrow$ F transition rather than the emergence of one of the SPs the free flow is recovered in the vicinity of the on-ramp.

(7) If q_{on} decreases, the GP either dissolves or it transforms into one of the SPs (between the boundaries $F_S^{(B)}$ and $S_J^{(B)}$) (item (6)).

(8) The discharge flow rate $q_{\text{out}}^{(\text{bottle})}$, i.e. the flow rate downstream of the on-ramp, depends on the type of congested pattern which is formed upstream of the on-ramp, on the pattern parameters and on the flow rate q_{on}. For example, for the GP in figure 2(*b*) the discharge flow rate $q_{\text{out}}^{(\text{bottle})} \approx 2030$ vehicles h^{-1}, for the WSP in figure 2(*d*) $q_{\text{out}}^{(\text{bottle})} \approx 2250$ vehicles h^{-1} and for the LSP in figure 2(*e*) $q_{\text{out}}^{(\text{bottle})} \approx 2150$ vehicles h^{-1}. In all these cases, $q_{\text{out}}^{(\text{bottle})}$ is higher than the flow rate out from the wide jam $q_{\text{out}} = 1810$ vehicles h^{-1}.

(iii) Within *the fundamental diagram approach* a diagram of congested patterns at on-ramps has recently been derived for a wide class of traffic flow models [8]. Both the diagram in figure 2(*a*) and nonlinear features of congested patterns in figures 2(*b*)–(*f*) are qualitatively different from the results in [2, 8]. These differences are summarized below in (1)–(6).

(1) In the diagram of congested states based on the fundamental diagram approach [2, 8–10], at the *highest* values of the flow rate to the on-ramp q_{on} the homogeneous congested pattern (HCT), i.e. a region of homogeneous traffic flow of very high density and low vehicle speed upstream of the on-ramp widening over time, occurs. WSP (figure 2(*d*)) at first sight looks like HCT in [2, 8]. However, in contrast to HCT, which occurs at very *high* flow rates to the on-ramp q_{on} only, in our model (figure 2(*a*)) the widening synchronized flow pattern (WSP) occurs at *low* values of the flow rate to the on-ramp q_{on} only.

As a result, features of the WSP and HCT are totally different: whereas the HCT is related to stable equilibrium states on the fundamental diagram of a traffic flow model where the vehicle speed is *very low* and the density is very high [2, 8, 10], the WSP in our model, in contrast, is related to a part of a two-dimensional region of states of synchronized flow of *high* vehicle speeds and low densities.

(2) In [2, 8], if the flow rate q_{on} continuously increases starting from $q_{\text{on}} = 0$ and the flow rate on the road q_{in} upstream of the on-ramp remains given and high enough, first triggered stop-and-go traffic (TSG) occurs where no synchronized flow can be formed, then oscillating patterns (OCT) appear where no wide moving jams can be formed, and finally HCT occurs. In contrast, in the diagram in figure 2(*a*), the GP which occurs at high enough q_{on} does *not* transform into another type of pattern at any possible high flow rate q_{on}.

(3) Besides, the GP shows a qualitatively different behaviour from both TSG and OCT in [2, 8]. Either free or synchronized flow can occur between the wide moving jams in the GP (figure 3(*a*)), whereas in TSG there is only free flow between moving jams. In contrast to the GP, OCT does not contain the subsequence of wide moving jams and the amplitude of speed oscillations in OCT decreases with increasing q_{on}. Thus, in our model there are *no* TSG and *no* OCT patterns.

(4) In [2, 8], if q_{on} decreases, then depending on q_{in}, instead of TSG also the pinned localized cluster (PLC) or the moving localized cluster (MLC) may occur, i.e. either pinned or moving jams of very high density and very low speed. This is in contrast to our diagram in figure 2(*a*): if q_{on} decreases, one of the synchronized flow patterns (either MSP or WSP or else LSP) can occur where the density is much lower and the speed is much higher than inside either synchronized flow of the GP or inside any moving jams.

Thus even the LSP, which at first sight looks like the PLC, has a different nonlinear nature from the PLC in [2,8]. The latter can also be seen if one notes that in [2,8] at low values q_{in} and high enough q_{on} where the PLC exists, the PLC always transforms into HCT if the flow rate q_{on} further increases. In contrast, in our approach if the flow rate q_{on} increases, the LSP either remains LSP at any high possible q_{on} (between the boundaries $F_S^{(B)}$ and $S_J^{(B)}$ in figure 2(*a*)) or the LSP transforms into the GP (right of the boundary $S_J^{(B)}$).

(5) In the diagram of congested patterns at on-ramps in [2, 8], near the boundary which separates TSG and OCT a congested pattern which is a mixture of TSG and OCT can occur, which has been used in [2, 10] for an explanation of the pinch effect observed in [5]. This mixture of TSG and OCT at first sight looks like the GP. However, this mixture pattern in [2,10] does not have its own region in the diagram of states because it transforms either into TSG if q_{on} decreases or into OCT if q_{on} increases. In our model, as has already been mentioned, there is no TSG and no OCT. As a result, the GP exists in a very large range of flow rates q_{on} and q_{in}. At a given q_{in}, the GP does not transform into another congested pattern even if q_{on} increases up to the highest possible values (figure 2(*a*)). Thus, the GP in our model has totally different features from the mixture of TSG and OCT in [2, 10].

(6) The DGP at first sight looks like the moving localized cluster (MLC) in [2, 8, 20]. However, the MLC occurs in initial free flow near the on-ramp and then it propagates upstream of the on-ramp leading to free flow conditions at the on-ramp. In contrast, in the DGP, the widening upstream region of the synchronized flow occurs first, then one or several wide moving jams emerge in this synchronized flow at large distances upstream of the on-ramp and finally synchronized flow can remain at the on-ramp (figure 2(*c*)).

The MSP (figures 2(*f*) and 3(*c*)) at first sight looks like the MLC in [2, 8, 20]. However, inside the MLC the vehicle speed and the flow rate are very low (down to zero). In contrast, inside the MSP the vehicle speed is high (60–90 km h^{-1}) and the flow rate is almost as high as in free flow conditions. Besides, in contrast to the MLC, the velocity of the downstream front of the MSP is not a characteristic parameter. At given model parameters this velocity for the MSP can change in a wide range.

To conclude, in our model based on three-phase-traffic theory [5, 18] both the diagram of congested patterns and the features of the patterns are totally different from those in models based on the fundamental diagram approach [2, 8–10, 20].

We thank Dietrich Wolf for discussion and for helpful suggestions and the German Ministry of Education for the financial support within the BMBF project 'DAISY'.

References

[1] Chowdhury D, Santen L and Schadschneider A 2000 *Phys. Rep.* **329** 199
[2] Helbing D 2001 *Rev. Mod. Phys.* **73** 1067 (cond-mat/0012229)
[3] Kerner B S 2001 *Networks Spatial Economics* **1** 35
[4] Kerner B S and Rehborn H 1996 *Phys. Rev.* E **53** R4275
[5] Kerner B S 1998 *Phys. Rev. Lett.* **81** 3797
Kerner B S 1999 *Phys. World* **12** 25
[6] Kerner B S 2000 *Transp. Res. Record* **1710** 136

[7] Kerner B S 2000 *J. Phys. A: Math. Gen.* **33** L221
[8] Helbing D, Hennecke A and Treiber M 1999 *Phys. Rev. Lett.* **82** 4360
[9] Lee H Y, Lee H W and Kim D 1999 *Phys. Rev.* E **59** 5101
[10] Treiber M, Hennecke A and Helbing D 2000 *Phys. Rev.* E **62** 1805
[11] Treiber M and Helbing D 1999 *J. Phys. A: Math. Gen.* **32** L17–23
Nelson P 2000 *Phys. Rev.* E **61** R6052
Lubashevsky I and Mahnke R 2000 *Phys. Rev.* E **62** 6082
[12] Krauß S, Wagner P and Gawron C 1997 *Phys. Rev.* E **53** 5597
[13] Tomer E, Safonov L and Havlin S 2000 *Phys. Rev. Lett.* **84** 382
[14] Knospe W, Santen L, Schadschneider A and Schreckenberg M 2000 *J. Phys. A: Math. Gen.* **33** L477
[15] Knospe W, Santen L, Schadschneider A and Schreckenberg M 2002 *Phys. Rev.* E **65** 015101(R) (cond-mat/0107051)
[16] Barlovic R, Santen L, Schadschneider A and Schreckenberg M 1998 *Eur. J. Phys.* B **5** 793
[17] Nagel K, Wolf D E, Wagner P and Simon P 1998 *Phys. Rev.* E **58** 1425
[18] Kerner B S 1998 *Proc. 3rd Symp. on Highway Capacity and Level of Service* vol 2, ed R Rysgaard (Ministry of Transport Road Directorate, Denmark) pp 621–42
Kerner B S 1999 *Transp. Res. Record* **1678** 160–7
Kerner B S 2002 *Preprints Transportation Research Board 81st Annu. Meeting, TRB Paper* 02-2918 (Washington, DC: Transportation Research Board)
[19] Rickert M, Nagel K, Schreckenberg M and Latour A 1996 *Physica* A **231** 534
[20] Kerner B S, Konhäuser P and Schilke M 1995 *Phys. Rev.* E **51** 6243–6